Clinical Cancer Research

Acquired *MET* Y1248H and D1246N Mutations Mediate Resistance to MET Inhibitors in Non–Small Cell Lung Cancer

Anna Li[1], Jin-ji Yang[1], Xu-chao Zhang[1], Zhou Zhang[2], Jian Su[1], Lan-ying Gou[1], Yu Bai[3], Qing Zhou[1], Zhenfan Yang[3], Han Han-Zhang[2], Wen-Zhao Zhong[1], Shannon Chuai[2], Qi Zhang[1], Zhi Xie[1], Hongfei Gao[1], Huajun Chen[1], Zhen Wang[3], Zheng Wang[1], Xue-ning Yang[1], Bin-chao Wang[1], Bin Gan[1], Zhi-hong Chen[1], Ben-yuan Jiang[1], Si-pei Wu[1], Si-yang Liu[1], Chong-rui Xu[1], and Yi-long Wu[1]

Abstract

Purpose: *MET* amplification, responsible for 20% of acquired resistance to EGFR tyrosine kinase inhibitor (TKI) in patients with advanced non–small cell lung cancer (NSCLC), presents an attractive target. Numerous studies have conferred susceptibility of *MET* mutations and focal amplification to targeted MET-TKIs. However, the mechanism underlying MET-TKIs–induced resistance remains elusive.

Experimental Design: We conducted a cohort of 12 patients with advanced NSCLC who developed resistance to a combinatorial therapy consisting of gefitinib and a type I MET-TKI. We performed capture-based targeted ultra-deep sequencing on serial tumor biopsies and plasmas ctDNA samples to detect and quantify genetic alterations.

Results: We identified 2 newly acquired *MET* mutations, Y1248H and D1246N, in 2 patients and further confirmed their resistance against type I MET-TKIs *in silco*, *in vitro*, and *in vivo*. Interestingly, NIH3T3 cells harboring either mutation exhibited responses to type II MET-TKIs, suggesting sequential use of MET-TKIs may offer a more durable response. In addition, we also discovered that EGFR amplification may act as an alternative MET-TKI resistance mechanism.

Conclusions: Our study provides insight into the diversity of mechanisms underlying MET-TKI–induced resistance and highlights the potential of sequential use of MET-TKIs. *Clin Cancer Res; 23(16); 4929–37. ©2017 AACR.*

Introduction

The paradigm for the pharmacologic management of non–small cell lung cancer (NSCLC) has revolutionized by the development of EGFR inhibitors. Concomitant with the exciting advancements in this field is the emergence of drug resistance (1–3), with the substitution of methionine for threonine at position 790 (T790M) being the most commonly acquired resistance mutation, accounting for approximately 50% of resistant cases. It can be successfully treated with third-generation tyrosine kinase inhibitors (TKI; ref. 2). *MET* amplification, responsible for 20% of EGFR-TKI–induced resistance, is a second well-established resistance mechanism known to bypass EGFR inhibition (4). Numerous studies have conferred susceptibility of *MET* mutations and focal amplification to targeted MET inhibitors (5, 6). *MET* is a receptor tyrosine kinase, activated by the binding of HGF, resulting in the phosphorylation of HER3 and subsequent activation of PI3K pathway, promoting cell proliferation, survival, mobility, migration, and epithelial to mesenchymal transition (7, 8). Gain-of-function alterations in MET, achieved through receptor overexpression, amplification, mutations, or alternative spicing, have been observed in many cancers, including NSCLC (9, 10).

MET has long been a candidate target for therapeutic development. A number of MET inhibitors, currently in clinical trials, have shown promising outcomes in NSCLC (11). Crizotinib, approved by the FDA for patients with NSCLC harboring anaplastic lymphoma kinase (ALK) rearrangements, was originally developed as a MET inhibitor (8, 12). Numerous studies have reported that patients harboring mutations in the *MET* exon 14 splice sites derived clinical benefits from crizotinib (5, 6, 13). The National Comprehensive Cancer Network guidelines recommend crizotinib to NSCLC patients harboring high-level *MET* amplification or *MET* exon 14 skipping mutation (5, 6, 14, 15). INC280, developed for tumors bearing MET overexpression or amplification, competes for the ATP-binding site in the tyrosine kinase domain, thus preventing activation of c-MET and the subsequent recruitment of downstream effectors (16, 17). In the ongoing Phase I INC280 clinical trial at our hospital, it induces durable response

[1]Guangdong Lung Cancer Institute, Guangdong General Hospital, and Guangdong Academy of Medical Sciences, Guangzhou, P.R. China. [2]Burning Rock Biotech, Guangzhou, Guangdong Province, P.R. China. [3]Asia Innovative Medicines and Early Development, AstraZeneca, Shanghai, China.

Note: Supplementary data for this article are available at Clinical Cancer Research Online (http://clincancerres.aacrjournals.org/).

A. Li, J.-j. Yang, X.-c. Zhang, and Z. Zhang contributed equally to this article.

Corresponding Author: Yi-long Wu, Guangdong Lung Cancer Institute, Guangdong General Hospital, and Guangdong Academy of Medical Sciences, 106 Zhongshan 2nd Road, Guangzhou 510080, P.R. China. Phone: 8620-8387-7855; Fax: 8620-8382-7712; E-mail: syylwu@live.cn

doi: 10.1158/1078-0432.CCR-16-3273

Translational Relevance

MET amplification, responsible for 20% of EGFR-tyrosine kinase inhibitor (TKI)–induced resistance, is a second well-established resistance mechanism known to bypass EGFR inhibition. Several structurally distinct MET inhibitors are under clinical development for treatment of non–small cell lung cancer (NSCLC). Numerous studies have conferred susceptibility of *MET* mutations and focal amplification to targeted MET-TKIs. However, the mechanism underlying MET-TKI–induced resistance remains elusive. We reveal that acquired *MET* Y1248H and D1246N mediate resistance to type I MET-TKIs from a cohort of 12 advanced NSCLC patients who developed resistance to gefitinib and were subsequently switched to a combinatorial therapy consisting of gefitinib and an MET-TKI. We further confirm their resistant effects both *in vitro* and *in vivo*. Interestingly, both mutations are not resistant to type II MET-TKIs, suggesting sequential use of MET-TKIs may offer a more durable response.

in EGFR-mutant lung cancer patients with acquired resistance to EGFR-TKIs, with preliminary 31% (28/90 patients) unconfirmed responsive rate (RR; ref. 18). Both crizotinib and INC280 are type I MET inhibitors, which preferentially bind the active conformation of MET. In contrast, type II MET inhibitors, such as cabozantinib (XL184), bind the inactive conformation (11). Although drug resistance associated with MET-TKIs has also been reported, there are limited studies investigating the underlying mechanisms. A recent study reported an acquired mutation *MET* D1228N (D1246N) in the kinase domain at time of progression of a patient exposed to crizotinib (19). Other mutations, including Y1230 (Y1248) occurring at the *MET* activation loop, have also been shown to have inhibitory effects against MET inhibitors *in vitro* (20, 21).

In this study, we conduct a cohort of 12 advanced NSCLC patients who developed resistance to gefitinib and were subsequently switched to a combinatorial therapy consisting of gefitinib and a MET-TKI. We provide insight into the diversity of mechanisms underlying MET inhibitors induced resistance by identifying two mutually exclusive mechanisms: EGFR amplification and *MET* mutations Y1248H and D1246N.

Materials and Methods

Patient selection and sample collection

Twelve NSCLC patients who harbored MET overexpression and developed resistance to MET inhibitor underwent tumor biopsy between April 2012 and January 2016. MET expression was detected by immunohistochemistry (IHC; antibody SP44). A minimum of 50% tumor cells with moderate or strong staining was defined as MET positive. Copy numbers were detected by FISH (By Cappuzzo scoring system & MET/CEP7 ratio). A minimum of 5 copies were required to be identified as positive or a MET/CEP7 ratio $\geq$1.8 was defined as c-MET amplification (low: 1.8–2.2, intermediate: 2.2–5, high: $\geq$5). Met probes were purchased from KREATECHTM. Patients were either treated in a clinical trial investigating the combinatorial effect of gefitinib and INC280 ($n = 11$) or with gefitinib and crizotinib ($n = 1$). Standard histopathology was performed to confirm the diagnosis of malignancy and histologic subtype. Tumor biopsies were obtained under an Institutional Review Board–approved protocol. All patients provided written informed consent.

Targeted DNA sequencing for plasma samples

Ten milliliter of whole blood was collected in K3EDTA-containing tubes (Cell-Free DNA BCT) and centrifuged at 2,000 *g* for 10 minutes at +4°C within 72 hours after collection. Supernatant was transferred to a fresh 15 mL centrifuge tube without disturbing the buffy coat layer and subjected to an additional centrifugation for 10 minutes at 16,000 *g* at +4°C. The supernatant was again transferred to a new tube. The plasma was stored at −80°C until further analysis. Circulating cell-free DNA was extracted from plasma samples using the QIAamp Circulating Nucleic Acid Kit (Qiagen) according to the manufacturer's instructions. Quantification of cell-free DNA (cfDNA) was performed using the Qubit 2.0 Fluorometer with the dsDNA HS assay kits (Life Technologies).

Tissue DNA extraction

DNA was extracted using the QIAamp DNA FFPE tissue Kit (Qiagen) according to the manufacturer's instructions. DNA concentration was measured using Qubit dsDNA assay.

Capture-based targeted DNA sequencing

Genetic profiles of all tissue samples were assessed by performing capture-based targeted deep sequencing using the OncoScreen panel (Burning Rock Biotech Ltd.), covering 2.02 MB of human genomic regions, including all exons and critical introns of 295 genes. DNA quality and size were assessed by high sensitivity DNA assay using a bioanalyzer. cfDNA samples were profiled using LungPlasma panel covering selected exons and introns of 168 genes, spanning 160 KB of human genomic regions. All indexed samples were sequenced on a NextSeq 500 (Illumina, Inc.) with pair-end reads.

Sequencing data analysis

The sequencing data in the FASTQ format were mapped to the human genome (hg19) using BWA aligner 0.7.10. Local alignment optimization, variant calling, and annotation were performed using GATK 3.2, MuTect, and VarScan, respectively. DNA translocation analysis was performed using both Tophat2 and Factera 1.4.3. Gene-level copy-number variation was assessed using a *t* statistic after normalizing reads depth at each region by total reads number and region size, and correcting GC-bias using a LOESS algorithm.

Sanger validation for *MET* mutation

Genomic DNA from each sample was used for sequence analysis of *MET* exon 19. These exons were amplified by PCR, and the resulting PCR products were purified and labeled for sequencing using the BigDye 3.1 Kit (Applied Biosystems) according to the manufacturer's protocols. Samples were ran on an ABI 3100 Genetic Analyzer (Applied Biosystems).

Droplet digital PCR validation for *MET* mutation

Droplet Digital PCR (ddPCR) was performed on a Bio-Rad QX100 ddPCR instrument. *MET* D1246N (G>A) primers and probes were purchased from Life Technologies. Sequences are

available upon request. The following PCR conditions were used: 1 cycle of 95°C × 10 minutes, 40 cycles of 95°C × 15 seconds, and 55°C × 1 minute, followed by 4°C hold. *MET* mutation–specific signals are generated in the VIC channel, whereas the *MET* wild-type (WT) signals are in the FAM channel. The quantification of the target molecule was presented as number of total copies (mutant plus WT) per sample in each reaction. Fractional abundance (F.A.) is calculated as follow: F.A. % = $(N_{mut}/(N_{mut}+N_{wt}) \times 100)$, where N_{mut} is the number of mutant events and N_{wt} is the number of WT events per reaction. ddPCR analysis of normal control DNA (genomic DNA) and no DNA template controls were always included.

Cell culture, transfection, plasmids, and virus packaging

NIH3T3 cell line was obtained from the American Type Culture Collection (ATCC). Cells were grown in DMEM (GIBCO-Invitrogen) supplemented with 10% NCBS and maintained at 37°C in a humidified atmosphere at 5% CO_2. pBabe puro c-MET WT was a gift from Joan Brugge (Addgene plasmid #17493). The *MET* sequence was cloned into the pMT143 lentiviral vector and was driven by a CMV7 promoter (Sunbio, plasmid#PSE2209). Two point mutation vectors (D1226N,Y1228H) were constructed based on PSE2209. All vectors were verified by DNA sequencing. Lentivirus particles were packaged and purified by Sunbio lentiviral system. NIH3T3 cells infected with lentivirus containing *MET*-WT and *MET*-Mutants were selected with 2 μg/mL puromycin for 5 days to obtain stable expression of indicated protein and kept in 1 μg/mL puromycin. All cell lines tested Mycoplasma negative (Mycoplasma Detection Kit; Cat. SE000-8010; Sesh-Biotech) within 6 months of performing the experiments. Cell line authentication was performed.

Protein detection

GAPDH was used as a loading control. The Akt, phospho-Akt (S473), Erk1/2, phospho-Erk1/2(T202/Y204), MET(D1C2,25H2), phospho-MET (Y1234/Y1235), S6 ribosomal protein (54D2), phosphor-S6 ribosomal protein (ser235/236), and phosphor-p70 S6 Kinase(Thr421/Ser424) antibodies were purchased from Cell Signaling Technology. All antibodies were used at a 1:1,000 dilution, except for GAPHD antibody, which was used at 1:10,000 dilution.

Cell viability assay

NIH3T3 cells (1,000) were plated in a 384-well plate and treated with indicated concentrations of INC280, crizotinib, or 0.1% DMSO for 72 hours. Cell survival was measured by MTS assay (G3580; Promega) following the manufacturer's instructions. Relative cell survival rate was normalized to the DMSO-treated group. Each data point represents the average of biological duplicates.

Effects of type I and type II MET-TKIs on tumor xenografts

To establish tumor xenografts, MET-mutants cells (1×10^6) were subcutaneously inoculated in the right hind of flank of female nu/nu athymic nude mice (6–8 weeks old) individually. After tumors reached a mean volume of 150 mm^3, mice were randomized ($n = 5$ per group) and orally administered INC280 (30 mg/kg twice daily), crizotinib (100 mg/kg/d), XL184 (20, 60 mg/kg/d), or vehicle for 14 days. Tumor size was measured 2 to 3 times weekly by caliper. Tumor volume was calculated using the following formula: Tumor volume = (length × width^2) × 0.5. Mice were sacrificed when tumor volume reached 2,000 mm^3 according to the principle of animal welfare. All experiments were performed following protocols approved by the Institutional Animal Care and Use Committee.

Due to the rapid progression of the tumors in vehicle, INC280, or crizotinib-treated groups, mice reached the maximum tumor volume prior to the scheduled treatment endpoints. Therefore, we had to terminate drug administration on the indicated days, according to the principle of animal welfare. So the values of percentage of tumor growth were calculated on the indicated days by comparing tumor volumes in drug-treated and vehicle-treated groups. * indicates $P < 0.05$ (Mann–Whitney *U*).

Results

Mutation spectrum

To elucidate potential mechanisms of resistance associated with MET-TKIs, we conducted a cohort of 12 patients with advanced NSCLC who showed MET overexpression after the development of resistance to gefinitib and were subsequently switched to a combinatorial regimen consisting of gefinitib and a type I MET-TKI. We performed capture-based targeted sequencing on serial tumor biopsies and blood samples using OncoScreen and LungPlasma panels, respectively, to detect and quantify genetic alterations. The OncoScreen panel, spanning 2.024 MB of human genome, consists of all exons and critical introns of 295 genes; LungPlasma panel, spanning 160 KB of human genome, consists of critical exons and introns of 168 genes.

At baseline, all patients harbored somatic *EGFR*-activating mutations confirmed by both ARMS-PCR and next-generation sequencing (NGS): 7 patients carried *EGFR* exon 19 deletions and the remaining 5 patients harbored *EGFR* exon 21 L858R substitutions. They were initially treated with gefitinib, an EGFR-TKI. After the emergence of drug resistance, they were subsequently switched to a combinatorial regimen consisting of gefitinib and a type I MET-TKI based on the detection of MET overexpression in tissue biopsy samples by IHC. One patient was treated with gefitinib and crizotinib; the remaining 11 patients were treated with gefitinib and INC280. Our NGS results revealed acquired *MET* amplification after developing resistance to gefitinib in half of the patients (6/12). Based on our NGS results, among 7 patients achieved partial response (PR), 5 of them harbored *MET* amplification prior to MET-TKI treatment; in contrast, among 5 patients achieved stable disease (SD) or progressive disease (PD), only 1 patient harbored *MET* amplification, suggesting the existence of other resistance mechanisms in patients achieved SD and PD despite the fact that they showed MET overexpression by IHC. Furthermore, this result suggested that utilizing NGS to interrogate *MET* amplification is a better predictive method. Interestingly, most patients achieved PR (5/7) harbored *EGFR* L858R at baseline; on the other hand, all SD and PD patients harbored *EGFR* exon 19 deletions at baseline, suggesting patients with baseline *EGFR* L858R mutations are more likely to respond to the combinatorial treatment ($P = 0.028$, Fisher exact test; Fig. 1).

T790M evolution

Although all enrolled patients tested negative for *EGFR* T790M mutation by ARMS-PCR prior to the combinatorial treatment, NGS still revealed 4 patients, who harbored T790M mutation. Three of them (P06, P09, and P11) belonged to the SD or PD group, and 1 patient (P05) belonged to the PR group. Prior to the

	Patient	P02	P04	P01	P03	P05	P10	P12	P06	P09	P07	P08	P11
Clinical information	Age(Yr)	32	63	67	61	50	48	44	57	36	62	45	54
	Gender	F	F	F	M	F	M	F	M	M	F	M	F
	Histologic type	ADC	ADC	ADC	ADC	ADC	ADC	ADC	ADC	ADC	ADC	ADC	ADC
	Treatment	G+C	G+I	G+I	G+I	G+I	G+I	G+I	G+I	G+I	G+I	G+I	G+I
	Best response	PR	PR	PR	PR	PR	PR	PR	SD	SD	PD	PD	PD
	PFS(month)	8.8	7.2	12.0	5.0	5.7	5.6	7.8	5.7	5.6	1.0	1.0	1.9
	EGFR sensitizing mutation	L858R	19del	L858R	L858R	L858R	19del	L858R	19del	19del	19del	19del	19del
MET Assessment before MET-TKI	MET_IHC(++~+++)	25%+++, 35%++	80%+++	55%++	60%+++	60%+++, 40%++	100%+++	95%+++, 5%++	55%+++	70%+++, 20%++	70%++	95%+++, 5%++	50%+++, 50%++
	MET_FISH	+	+	+	+	-	+	NA	+	+	-	+	+
	MET_NGS	3.6	3.9	-	3.9	-	2.9	8.2	-	-	NA	-	3.9
Major genetic change after MET-TKI	MET mutation	Y1248H	D1246N										
	EGFR CN increase after MET TKI	0.9	1.3	1.5	2.8	3.1	15.1	0.7	1.1	1.0	NA	1.2	0.6
T790M Evolution	T790M baseline	0.0%	0.0%	0.0%	NA	0.0%	NA	NA	10.7%	0.0%	0.0%	0.0%	NA
	T790M after EGFR TKI	0.0%	0.0%	0.0%	0.0%	9.5%	0.0%	23.7%	1.5%	30.9%	NA	0.0%	10.0%
	T790M after MET TKI	0.0%	5.2%	14.1%	0.0%	11.5%	10.2%	NA	4.8%	35.7%	4.2%	13.4%	2.7%
	T790M after MET TKI (ctDNA)	3.1%	4.8%	NA	0.0%	1.7%	8.4%	7.0%	1.2%	26.3%	NA	12.0%	4.4%

ADC: Adenocarcinoma
G+C: Gefitinib+Crizotinib. G+I: Gefitinib+INC280
BR: Best response. PR: Partial response.
SD: Stable disease. PD: Progressed disease
CN: gene copy number estimated by NGS.
NA: data not available

Figure 1.
Clinical features and mutation spectrum. Basic clinical information and major genetic aberrations are summarized in this table. Eleven patients were treated with gefitinib and INC280; 1 patient was treated with gefitinib and crizotinib. Seven achieved PR, 2 achieved SD, and 3 had PD. BR, best response; PFS, progression-free survival.

combinatorial treatment, 6 of 7 patients were T790M negative in the PR group; in contrast, in SD and PD group, only 1 of 4 patients was T790M negative (Fisher exact test: $P = 0.088$, OR = 12.2), suggesting T790M is a possible concurrent resistance mechanism. The Student *t* test shows a marginal difference between patients harboring T790M mutation and those without it prior to the combinatorial treatment, as demonstrated in the Kaplan–Meier curves (Supplementary Fig. S1), although it did not reach statistical significance. The allele frequency (AF) of T790M has increased during the course of combinatorial treatment for a majority of patients who carried T790M prior to the combinatorial treatment except for 1 patient (P11). In addition, 2 patients (P01 and P10) developed *de novo* T790M mutation after the combinatorial treatment (Fig. 1). Collectively, our result indicates that among patients who presented *MET* amplification as a resistance mechanism to gefitinib, it is not unlikely to have *EGFR* T790M as a concurrent resistance mechanism. Patients harboring both mutations are less likely to respond to the combinatorial treatment.

Emergence of secondary *MET* mutations: Y1248H and D1246N

At time of progressive disease, our NGS results revealed two newly acquired mutations at the kinase domain of *MET*, Y1248H and D1246N, from 2 patients whose best response was PR. Neither mutation was reported in treatment-naïve NSCLC patients from interrogating the Cancer Genome Atlas (TCGA) database. Both patients showed MET amplification after gefitinib treatment (Fig. 2F, G, M, and N). Patient 02, a 32-year-old female, whose cancer had progressed on multiple prior lines of treatments, demonstrated PR after 2 months of combinatorial treatment consisting of gefitinib and crizotinib (Fig. 2D); however, her CT scans revealed systemic progression after 8.8 months of treatment (Fig. 2E). NGS analysis of serial tissue biopsy and blood samples revealed two acquired *in trans MET* mutations, Y1248H and D1246N, at time of disease progression (Fig. 2A). *MET* Y1248H was detected in both tumor biopsy (AF = 20.8%) and blood sample (AF = 1.36%) taken after exposure to crizotinib; D1246N (AF = 1.51%) was only detected in the blood sample, indicating additional heterogeneity captured by liquid biopsy. Clonal progression analysis revealed the existence of *EGFR* L858R prior to the treatment of gefinitib followed by the subsequent development of *MET* amplification. After switching to the combinatorial treatment consisting of gefitinib and crizotinib, the patient acquired *de novo MET* Y1248H, D1246N, and *EGFR* T790M in addition to existing *MET* amplification and *EGFR* L858R (Supplementary Fig. S2A).

Patient 04, a 63-year-old female, demonstrated PR after 1 month of combinatorial treatment consisting of gefitinib and INC280 (Fig. 2K). She also developed systemic progression after 7.2 months of treatment (Fig. 2L). NGS analysis revealed a *MET* mutation D1246N occurring in exon 19, present in both tissue biopsy (AF = 5.21%) and blood samples (AF = 4.81% and 2.66%) taken at time of disease progression, but not before MET-TKI treatment (Fig. 2E). *MET* Y1248H from tumor biopsy

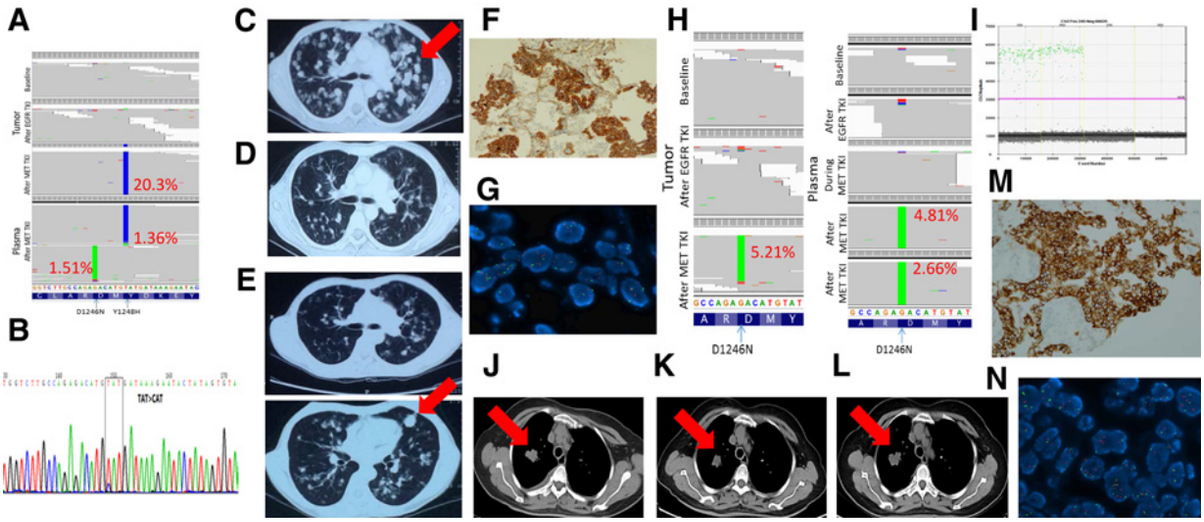

Figure 2.

Acquired resistance to INC280 and crizotinib mediated by acquired *MET* Y1248H and D1246N. **A,** In subject P02, targeted NGS revealed an acquired T→G mutation (blue) in both tumor biopsy and blood samples, and an acquired G→A mutation (green) in the blood sample only. **B,** Sanger sequencing validation of T→G mutation. **C–E**, CT scans at various time points: before treatment **(C)**, at best response (**D**), and at progressive disease (**E**). **F** and **G,** MET status assessed by IHC (25%+++; 30%++) and FISH (**G**: MET:CEP7 ratio = 2.8, copies 5.75) at PD after EGFR-TKI treatment. **H,** In subject P04, targeted NGS revealed an acquired G→A mutation (green) in both tumor biopsy and blood samples. **I,** ddPCR validation of the acquired G→A mutation. **J–L,** CT scans at various time points: before treatment (**J**), at best response (**K**), and at progressive disease (**L**). **M** and **N,** MET status assessed by IHC **(M**; 80%+++) and FISH (**N**; MET:CEP7 ratio = 1.2, copies 5.22) at PD after EGFR-TKI treatment.

of P02 and D1246N from both tissue and plasma samples of P04 after progression were successfully validated by Sanger sequencing and ddPCR, respectively (Fig. 2B and I). Clonal evolution for this patient is relatively simple, revealing the existence of *EGFR* 19del prior to gefitinib followed by acquired *MET* amplification. The combinatorial treatment induced *de novo MET* D1246N (Supplementary Fig. S2B).

In addition to *MET* mutations, acquired *EGFR* copy-number gain was also observed in 4 of 7 patients whose best response was PR. Patients with SD or PD as their best response did not harbor *EGFR* amplification (Fig 1). The other 2 patients whose best response was PR acquired secondary *MET* mutations, suggesting a mutually exclusive relationship between *MET* mutations and *EGFR* amplification. Unfortunately, we were unable to collect tissue biopsy from P12; therefore, EGFR copy-number difference cannot be calculated for this patient (Fig. 1).

MET mutations Y1248H and D1246N confer resistance *in vitro*, *in vivo*, and *in silico*

To confirm MET mutations mediated resistance against type I MET-TKIs, we stably expressed mouse *MET* Y1228H (equivalent to human Y1248H) and mouse *MET* D1226N (equivalent to human D1246N) individually in NIH3T3 cells (mouse embryonic fibroblasts) and assessed cell proliferation 72 hours after the treatment. Cells were treated with increasing concentration of either INC 280 or crizotinib. Both of them are type I MET-TKI. The growth rate of cells expressing WT *MET* was significantly inhibited upon either INC280 or crizotinib treatment. In contrast, mutant forms exhibited relatively sustained growth rate upon type I MET-TKI treatment (Fig. 3A and B). Both WT and mutant expressing cells were sensitive to XL184, a type II MET-TKI, exhibiting no difference in growth inhibition (Fig. 3C). To investigate the downstream effects of resistance to MET-TKIs, we examined the protein levels of key downstream effectors of MET and major cross-talk pathways' participants. We collected cell extracts at different inhibitor concentrations and assessed the total as well as the phosphorylated form of MET, AKT, ERK, S6, and S6K. Upon either INC280 or crizotinib treatment, cells expressing WT *MET* showed a downregulation of the phosphorylated form of the proteins assayed, reflecting its responsiveness to such inhibitor; in contrast, the expression level of total proteins remained constant. On the other hand, cells expressing either form of the mutants exhibited constant protein levels of both the phosphorylated forms and the nascent forms of downstream effector proteins, reflecting their resistance to such inhibitors (Fig. 3D and F). Upon XL184 treatment, both WT and mutant cells showed a downregulation of the phosphorylated forms of major downstream effectors proteins (Fig. 3F). Collectively, our Western blot results are in an agreement with our cell proliferation assays, demonstrating resistance against INC280 and crizotinib but not XL184.

To confirm that both mutations are resistant to type I MET inhibitors but sensitive to MET type II inhibitors, we treated cells expressing either mutant with two additional inhibitors, savolitinib, a type I MET-TKI or BMS777607, a type II MET-TKI. Both our cell proliferation assay and immunoblotting results are consistent with our previous results (Supplementary Fig. S3A–S3D). Cell growth rate was relatively sustained in mutant cell lines after savolitinib treatment; in contrast, upon BMX777607 treatment, the growth rates of both mutant cell lines were inhibited. Taken together, our results demonstrate that both *MET* mutations are resistant to type I MET-TKIs but remain sensitive to type II MET-TKIs.

Next, we investigated *MET* mY1228H and mD1226N (equivalent to human Y1248H and D1246N, respectively) mediated resistance *in vivo*. Cells expressing either mutant were inoculated into female nu/nu mice. When tumor reached 150 m^3, mice were

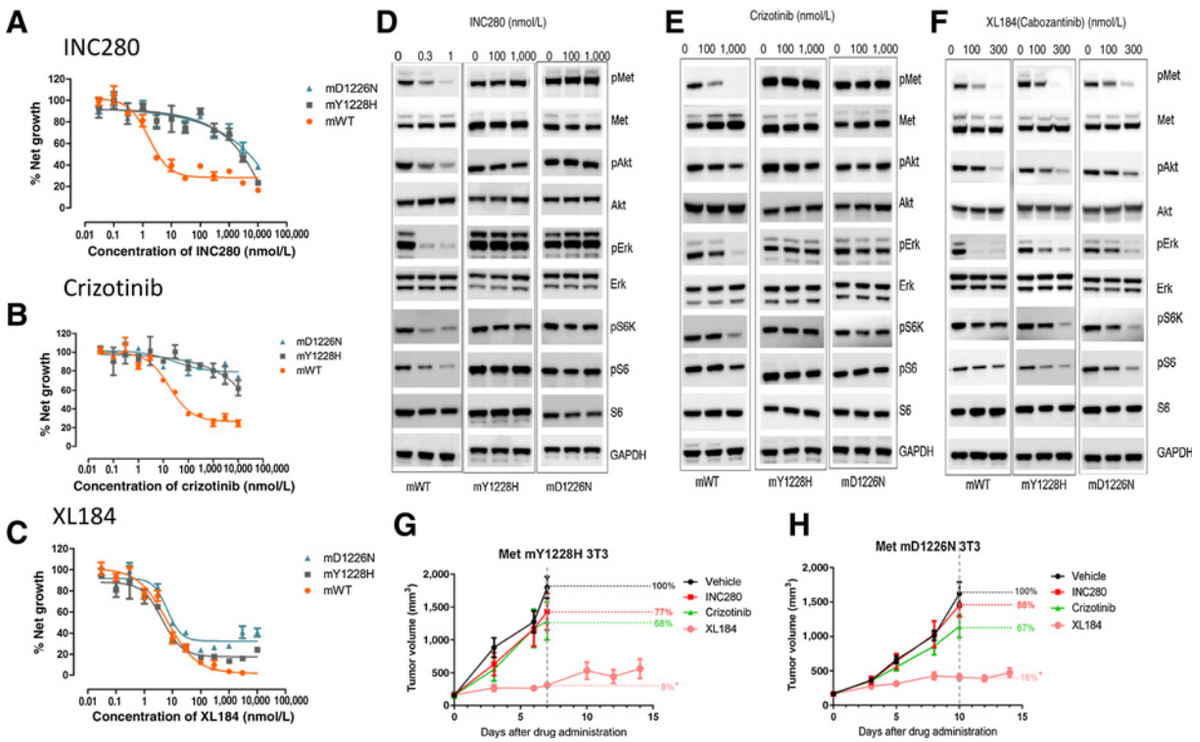

Figure 3

Functional validations of *MET* Y1248H and D1246N. **A–C,** NIH3T3 cells harboring either mouse MET Y1228H or mouse MET D1226N were treated with INC280 (**A**), crizotinib (**B**), or XL184 (**C**) at indicated concentrations. Viable cells were measured after 72 hours of treatment. Error bars represent SD of biological triplicates. **D–F,** After treatment with INC280 (**D**), crizotinib (**E**), and XL184 (**F**), cell extracts were immunoblotted to detect total protein levels and phosphorylated forms of key downstream effectors of MET and major cross-talk pathway participants. GAPDH is used as a loading control. **G** and **H,** Female nu/nu athymic nude mice bearing MET mY1228H (**G**) and MET mY1226N (**H**) were treated with vehicle, INC280 (30 mg/kg twice daily), crizotinib (100 mg/kg/d), or XL184 (60 mg/kg/d) for 14 days. Tumor volume was determined 2 to 3 times per week. Data represent the mean tumor volume (in mm^3) and standard error for each treatment group.

randomized (5 per group) and orally administered INC 280, crizotinib, XL 184, or vehicle. Only XL 184 treatment resulted in significant tumor growth inhibition. Upon XL 184 treatment, mice expressing *MET* mY1228H or mD1226N had an average tumor volume that was 8% or 16% of the vehicle-treated mice, respectively. In contrast, in mice bearing *MET* mY1228H or mD1226N, treatment with INC280 resulted in an average tumor volume that was 77% or 88% of the original tumor and treatment with crizotinib resulted in an average tumor volume that was 67% or 68% of the original tumor volume (Fig. 3G and H). Mice bearing *MET* mD1226N showed gradual body weight gain under all treatments. Mice bearing MET mY1228H showed gradual body weight gain after exposure to INC280 and XL184 at 5 mg/kg/d. The body weight of mice remained constant after exposure to crizotinib and XL184 at higher dose: 20 mg/kg/d and 60 mg/kg/d (Supplementary Fig. S4A and S4B) Furthermore, dose-dependent inhibition was observed when treating mice bearing *MET* mutations with increasing concentrations of XL184, ranging from 0 mg/kg/d to 60 mg/kg/d (nonlinear mixed-effect model, $P < 0.0001$; Supplementary Fig. S4C and S4D). The inhibition effect of XL184 progressively increases as the dosage increases.

Next, we performed molecular studies to investigate the conformational changes induced by two mutations: Y1248H and D1246N. WT *MET* allows INC280 and crizotinib to be bound properly, occupying the ATP-binding site and making contacts with neighboring proteins through hydrogen bonds and extensive hydrphobic interations. Mutant structures underwent distortion, thus abrogating the binding of INC280 and crizotinib and subsequently leading to drug resisitance (Fig. 4A–G). In contrast, the binding of XL184 does not involve the ATP-bidning site; therefore, both mutations failed to render inhibitory effect (Fig. 4C and F). The results from our ligand-binding studies agreed with results from both cell proliferation assays and electrophoresis.

Discussion

The realization that drug resistance inevitably arises has spurred great interest in elucidating resistance mechanisms. To the best of our knowledge, this is the first study interrogating resistant mutations induced by INC280 in patients. In this study, we investigated resistance to MET-TKIs and identified two acquired *MET* mutations Y1248H and D1246N. Neither was reported in treatment-naïve NSCLC patients from interrogating TCGA database. Subsequently, we confirmed their inhibitory activities both *in vitro* and *in silico*. Treatment of NIH3T3 cells stably expressing two mutants individually with type I inhibitors: INC280 or crizotinib but not type II inhibitor XL184 resulted in the maintenance of downstream PI3K-AKT and MEK-ERK signaling

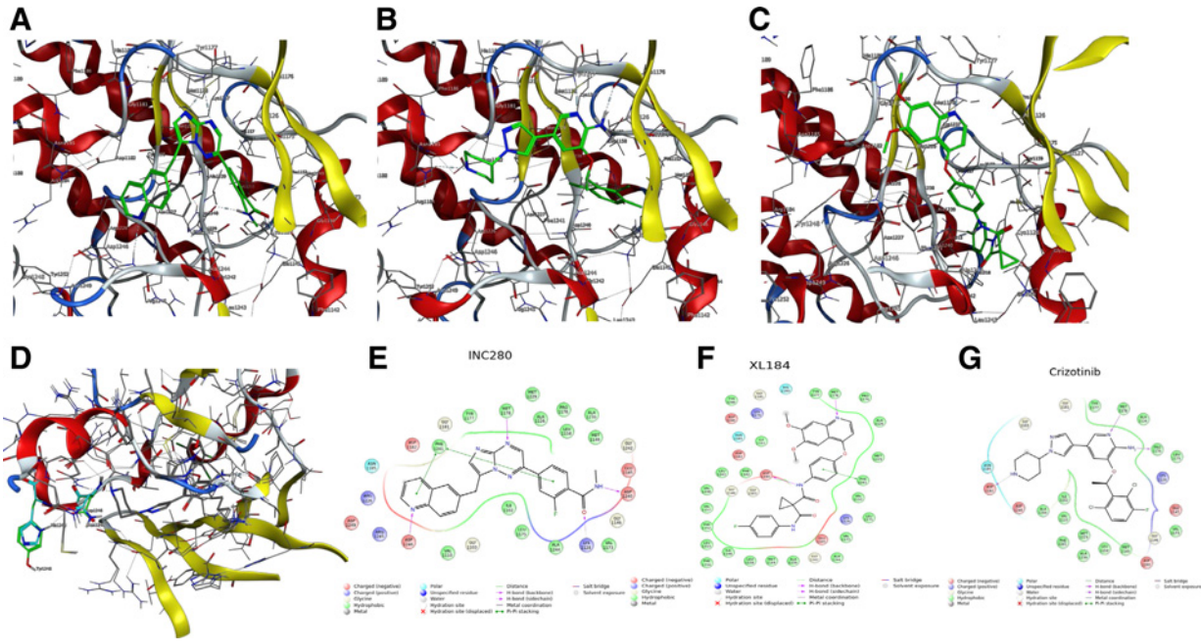

Figure 4.

Ligand interaction map. Molecular modeling studies show the interaction between WT *MET* with different MET inhibitors. **A,** docked INC280 in MET, imadazo triazine core formed hydrogen bindings to Hinge residue, Met1178. Amide bond formed hydrogen bonds to the Asp1240 from DFG loop and Lys1128 from K72. The benzamide part occupied the pocket next to the alpha-C helix. Phe1241 from DFG form stackings to benzamide ring on the right and quinoline rings on the left. **B,** Docked crizotinib in cMet, the pyridin-amine core formed hydrogen bonds to hinge residues, Met1178 and Pro1176. Tri-fluorobenzene sat on top of the DFG loop. Amine from piperidine formed a hydrogen bond to Asp1182. **C,** Docked XL184 in cMet, the quinoline core formed hydrogen bond to the hinge residue, Met1178. The central phenyl ring formed stackings to Phe1241 from DFG loop and amine formed hydrogen bond to Asp1240 from DFG loop. The fluorobezene occupied the pocket next to the alpha-C helix. **D,** Overlaid structures of two mutations, Y1248H and D1246N (cyan stick model), on the corresponding WT residues (green stick model). **E–G,** 2D structures of compounds in complex with Met.INC280 (**E**) and crizotinib (**F**) and XL184 (**G**).

pathways, indicating type II inhibitor such as XL184 might lead to a more durable response. This finding is in an agreement with a previous study, which found *MET* D1228N rendered resistance to NVP-BVU972, a type I MET inhibitor but not to AMG 458, a type II MET inhibitor (21). Furthermore, the sequential use of Met inhibitors has been reported. A patient was switched to a treatment consisting of an EFGR inhibitor and a type II MET inhibitor, cabozantinib, after developing an acquired mutation, MET D1228V, and demonstrated a dramatic response (22). We observed that even in WT *MET*, the type I inhibitors appear to be less effective than type II inhibitor (Fig. 3A to C). This can be potentially attributed to the differential binding affinities. Predicted binding affinity data revealed that cabozantinib is 10-fold more potent than the other two inhibitors. Furthermore, cabozantinib (MW: 501.513, Vol: 1515.029) is bigger than INC280 (MW: 412.425, Vol: 1273.715) and crizotinib (MW: 450.342, Vol: 1294.587), resulting in extending to and occupying the hydrophobic pocket next to the c alpha-Helix. Recently, two studies have reported two mutations at this residue: Heist and colleagues reported *MET* D1228N as an acquired resistance to crizotinib, and Bahcall and colleagues reported *MET* D1228V as an acquired resistance to type I MET inhibitors, suggesting this resistance mechanism will likely to impose a clinical problem (19, 22). A more comprehensive analysis of serial plasma and tumor biopsy samples is needed to elucidate the incidence rate of *MET* mutations Y1248H and D1246N. Efforts are needed to develop next-generation MET inhibitors.

Our study highlights a relatively underappreciated concept: heterogeneity associated with resistance mechanisms, and reveals the importance of recognizing such heterogeneity. Previous studies show that *MET* amplification often occurs independent of T790M mutation (2). Our study revealed 4 patients, among whom 3 of them belonged to the SD/PD group, harboring T790M mutation in conjunction with *MET* amplification after exposure to gefitinib, highlighting heterogeneity in resistance mechanisms. We observed that patients with multiple resistance mechanisms (T790M and *MET* amplification) showed inferior responses and shorter progression-free survival when treated with the combinatorial therapy. In these cases, INC280 may effectively suppress the growth of subclones harboring *MET* amplification, but a population of T790M-positive subclones may have a growth advantage, resulting in the progression of disease. Furthermore, T790M status evolves during the course of combinatorial treatment, necessitating continuous monitoring. Among the 6 patients who did not harbor T790M mutation prior to MET-TKI, 4 of them acquired such mutation during the course of combinatorial treatment. The AF of T790M has increased during the course of combinatorial treatment for a majority of patients who carried T790M prior to MET-TKI. Understanding the mechanisms of resistance facilitates categorizing patients for targeted therapy to maximize clinical benefits. A combinatorial treatment consists of MET-TKI, and AZD9291 may be more beneficial to patients harboring both T790M and *MET* amplification.

In addition to acquired *MET* mutations as resistance mechanisms to MET inhibitors, we observed *EGFR* amplification in 4 patients who achieved PR and had no *MET* mutation at PD after exposure to INC280 (Fig. 1), suggesting *EGFR* amplification might also confer INC280 resistance independent of *MET* mutations. Although *EGFR* amplification has never been associated with drug resistance, it has been reported to support metastatic progression of prostate cancer (23). More efforts are needed to validate its inhibition against MET-TKIs.

In this study, we observed some discordance between tissue biopsy and plasma samples. *MET* D1246N was not observed in the tissue biopsy but present in the plasma sample from patient 02. It has been well established that a single biopsy is not adequate in capturing the full scope of resistance mechanisms (24). The majority of cfDNA is released from apoptotic or necrotic tumor cells, thus reflecting the genetic profile of the tumor. The NGS-based cfDNA profiling assay enables us to visualize the entire mutation spectrum, thus paving the way for routine application of liquid biopsies in the clinic.

In summary, we demonstrate that *MET* mutations Y1248H and D1246N are resistance mechanisms for type I MET-TKIs. NIH3T3 cells expressing either mutation showed resistance to both INC280 and crizotinib but not cabozantinib, indicating the potential of sequential use of MET inhibitors may lead to a more durable response.

Disclosure of Potential Conflicts of Interest

C.-r. Xu reports receiving speakers bureau honoraria from AstraZeneca, Eli Lilly, Pfizer, and Roche, and holds ownership interest (including patents) in Illumina. Y.-l. Wu holds ownership interest (including patents) in AstraZeneca, Eli Lilly, and Roche, and is a consultant/advisory board member for AstraZeneca and Roche. No potential conflicts of interest were disclosed by the other authors.

Authors' Contributions

Conception and design: A. Li, J.-j. Yang, X.-c. Zhang, L.-y. Gou, Q. Zhou, Z. Yang, Z.-h. Chen, Y.-l. Wu

Development of methodology: A. Li, X.-c. Zhang, J. Su, L.-y. Gou, S. Chuai, Z. Xie, H. Gao, B. Gan, Z.-h. Chen

Acquisition of data (provided animals, acquired and managed patients, provided facilities, etc.): A. Li, X.-c. Zhang, L.-y. Gou, Q. Zhou, W.-Z. Zhong, Q. Zhang, Zhen Wang, X.-n. Yang, B.-c. Wang, B.-y. Jiang, C.-r. Xu, Y.-l. Wu

Analysis and interpretation of data (e.g., statistical analysis, biostatistics, computational analysis): A. Li, J.-j. Yang, X.-c. Zhang, Z. Zhang, J. Su, L.-y. Gou, Z. Yang, H. Han-Zhang, W.-Z. Zhong, S. Chuai, Q. Zhang, H. Chen, Zheng Wang, C.-r. Xu, Y.-l. Wu

Writing, review, and/or revision of the manuscript: A. Li, J.-j. Yang, X.-c. Zhang, Z. Yang, H. Han-Zhang, S. Chuai, Q. Zhang, Z.-h. Chen, C.-r. Xu, Y.-l. Wu

Administrative, technical, or material support (i.e., reporting or organizing data, constructing databases): A. Li, J.-j. Yang, X.-c. Zhang, Z. Zhang, W.-Z. Zhong, S. Chuai, C.-r. Xu

Study supervision: J.-j. Yang, Z. Yang, H. Gao, Z.-h. Chen, S.-p. Wu, S.-y. Liu, Y.-l. Wu

Other (participated in *in vitro* assay design): Y. Bai

Acknowledgments

The authors thank the patients and investigators for their participation in this study and Dr. Xiaotao Wang, former AstraZeneca scientist, who provided the scientific input in virus packaging work.

Grant Support

This study was supported by Guangzhou Science and Technology Bureau (grant no. 2014Y2-00545, Y.-l. Wu; grant no. 2011Y2-00014); Special Fund of Public Interest by National Health and Family Control Committee (grant no. 201402031, Y.-l. Wu); Key Lab System Project of Guangdong Science and Technology Department-Guangdong Provincial Key of Translational Medicine in Lung Cancer (grant no. 2012A06140006, Y.-l. Wu); and National Science Funding of China (grant no. 81472207).

The costs of publication of this article were defrayed in part by the payment of page charges. This article must therefore be hereby marked *advertisement* in accordance with 18 U.S.C. Section 1734 solely to indicate this fact.

Received December 31, 2016; revised December 20, 2016; accepted April 4, 2017; published OnlineFirst April 10, 2017.

References

1. Thress KS, Paweletz CP, Felip E, Cho BC, Stetson D, Dougherty B, et al. Acquired EGFR C797S mutation mediates resistance to AZD9291 in non-small cell lung cancer harboring EGFR T790M. Nat Med 2015; 21:560–2.
2. Tan CS, Gilligan D, Pacey S. Treatment approaches for EGFR-inhibitor-resistant patients with non-small-cell lung cancer. Lancet Oncol 2015;16: e447–59.
3. Yun CH, Mengwasser KE, Toms AV, Woo MS, Greulich H, Wong KK, et al. The T790M mutation in EGFR kinase causes drug resistance by increasing the affinity for ATP. Proc Natl Acad Sci U S A 2008;105:2070–5.
4. Engelman JA, Zejnullahu K, Mitsudomi T, Song Y, Hyland C, Park JO, et al. MET amplification leads to gefitinib resistance in lung cancer by activating ERBB3 signaling. Science 2007;316:1039–43.
5. Frampton GM, Ali SM, Rosenzweig M, Chmielecki J, Lu X, Bauer TM, et al. Activation of MET via diverse exon 14 splicing alterations occurs in multiple tumor types and confers clinical sensitivity to MET inhibitors. Cancer Discov 2015;5:850–9.
6. Paik PK, Drilon A, Fan PD, Yu H, Rekhtman N, Ginsberg MS, et al. Response to MET inhibitors in patients with stage IV lung adenocarcinomas harboring MET mutations causing exon 14 skipping. Cancer Discov 2015;5:842–9.
7. Blumenschein GRJr., Mills GBGonzalez-Angulo AM. Targeting the hepatocyte growth factor-cMET axis in cancer therapy. J Clin Oncol 2012; 30:3287–96.
8. Sadiq AA, Salgia R. MET as a possible target for non-small-cell lung cancer. J Clin Oncol 2013;31:1089–96.
9. Birchmeier C, Birchmeier W, Gherardi E, Vande Woude GF. Met, metastasis, motility and more. Nat Rev Mol Cell Biol 2003;4:915–25.
10. Gentile A, Trusolino L, Comoglio PM. The Met tyrosine kinase receptor in development and cancer. Cancer Metast Rev 2008;27:85–94.
11. Cui JJ. Targeting receptor tyrosine kinase MET in cancer: Small molecule inhibitors and clinical progress. J Med Chem 2014;57:4427–53.
12. Feng Y, Thiagarajan PSMa PC MET signaling: Novel targeted inhibition and its clinical development in lung cancer. J Thoracic Oncol 2012;7:459–67.
13. Drilon A, Somwar R, Wagner JP, Vellore NA, Eide CA, Zabriskie MS, et al. A novel crizotinib-resistant solvent-front mutation responsive to cabozantinib therapy in a patient with ROS1-Rearranged lung cancer. Clin Cancer Res 2016;22:2351–8.
14. National Comprehensive Cancer Network. NCCN Guidelines Version 4.2016 Non-Small Cell Lung Cancer; 2016. Available from: https://www.nccn.org/professionals/physician_gls/f_guidelines.asp.
15. Ou SH, Kwak EL, Siwak-Tapp C, Dy J, Bergethon K, et al. Activity of crizotinib (PF02341066), a dual mesenchymal-epithelial transition (MET) and anaplastic lymphoma kinase (ALK) inhibitor, in a non-small cell lung cancer patient with de novo MET amplification. J Thoracic Oncol 2011;6:942–6.
16. Moran-Jones K, Brown LM, Samimi G. INC280, an orally available small molecule inhibitor of c-MET, reduces migration and adhesion in ovarian cancer cell models. Sci Rep 2015;5:11749.
17. Liu X, Wang Q, Yang G, Marando C, Koblish HK, Hall LM, et al. A novel kinase inhibitor, INCB28060, blocks c-MET-dependent signaling, neoplastic activities, and cross-talk with EGFR and HER-3. Clin Cancer Res 2011;17:7127–38.

18. Wu YL YJ, Kim DW, Su WC, Ahn MJ, Lee DHSafety and efficacy of INC280 in combination with gefitinib (gef) in patients with EGFR-mutated (mut), MET-positive NSCLC: A single-arm phase lb/ll study. J Clin Oncol 2014;32:35s,(suppl; abstr 8017).
19. Heist RS, Sequist LV, Borger D, Gainor JF, Arellano RS, Le LP, et al. Acquired resistance to crizotinib in NSCLC with MET exon 14 skipping. J Thoracic Oncol 2016;11:1242–5.
20. Qi J, McTigue MA, Rogers A, Lifshits E, Christensen JG, Jänne PA, et al. Multiple mutations and bypass mechanisms can contribute to development of acquired resistance to MET inhibitors. Cancer Res 2011;71:1081–91.
21. Tiedt R, Degenkolbe E, Furet P, Appleton BA, Wagner S, Schoepfer J, et al. A drug resistance screen using a selective MET inhibitor reveals a spectrum of mutations that partially overlap with activating mutations found in cancer patients. Cancer Res 2011;71: 5255–64.
22. Bahcall M, Sim T, Paweletz CP, Patel JD, Alden RS, Kuang Y, et al. Acquired MET D1228V mutation and resistance to MET inhibition in lung cancer. Cancer Discov 2016;6:1334–41
23. Day KC, Hiles GL, Kozminsky M, Dawsey SJ, Paul A, Broses LJ, et al. HER2 and EGFR overexpression support metastatic progression of prostate cancer to bone. Cancer Res 2017;77:74–85.
24. Alix-Panabieres C, Pantel K. Clinical applications of circulating tumor cells and circulating tumor DNA as liquid biopsy. Cancer Discov 2016; 6:479–91.